



ANALYSIS OF THE UNCERTAINTY ASSOCIATED WITH NUMERICAL SCHEMES IN FLOOD INUNDATION MODELS

T D M Willis¹, N G Wright¹, P A Sleigh¹
¹*School of Civil Engineering, University of Leeds*

ABSTRACT: Recent evaluations of 2D models have focused on benchmarking computer codes and analysis of model outputs with respect to model inputs, focusing on the model as a black box, in order to understand sources of input uncertainty and how they propagate through to results. In this work, the influence of the numerical representation of the model on the results and the associated uncertainty is evaluated in a systematic way. For a test case of a canal embankment outburst event in Coventry the LISFLOOD code, which contains modules within the framework with different levels of physical representation, is tested against a range of uncertain inputs that are typically considered in a modeling exercise. The analysis is extended to show how traditional evaluation techniques such a comparison of extent do not capture the full uncertainty range of the modules. Instead, the use of risk based methods, in this case a cost of damage model shows how local variations in model results are rarely captured in measures of extents, but can be enhanced with exposure based methods. Overall, the level of physical representation is shown to be critical to model results.

1. INTRODUCTION

Uncertainty in flood inundation modeling is a critical area of contemporary research, in particular identifying the sources of uncertainty, how it propagates to output, and quantifying the effect of uncertainty in the model results. A number of studies have explored how uncertainty in model inputs such as Manning's friction parameter, cell size and inflow hydrographs contribute to model uncertainty (Aronica et al 2002, Hall et al 2005, Brandimarte et al 2010), but the contribution of the level of physical representation in the numerical model has not be explored as a source of uncertainty. The level of physical representation is defined as the number of terms from the governing equations incorporated into the numerical model. In order to overcome the computational cost of 2D Hydraulic modeling, a number of simplified approaches to solving the governing equations have been developed. Most prevalent amongst these is the LISFLOOD-FP code of Bates and De Roo (2000). This diffusion based code has been widely used in research (Fewtrell et al 2008, Pappenberger et al 2008), but the impact of using this approach becomes critical as grid cell sizes reduce to model urban areas (Fewtrell et al 2011). A number of comparison and benchmarking studies of these simplified approaches and full Shallow Water Equation (SWE) has been undertaken (Hunter et al 2008, Environment Agency 2010, 2012 and Neal et al 2011). These studies have provided insight into how simplified approaches and full SWE based models compare. Here this approach is extended to consider this impact in an uncertainty context, by comparing models with different level of physical representation to a number of inputs that are varied across their range of uncertainty. Each input is then cross compared in a systematic uncertainty analysis. In order to explore how critical this impact is and how it propagates through the modeling process, the cost of damage as a model output was calculated. By using a cost of damage method to explore model outputs, a secondary level of analysis was undertaken, where the uncertainty associated with model evaluation techniques could be assessed.

The LISFLOOD-FP code contains modules with different level of physical representation which provides a modeling framework to assess the impact of physical representation. A test case is then used to test different model inputs versus the level of physical representation. The test case is a historic canal embankment failure in Coventry, which provides a stringent test for hydraulic models as it contains both complex topography and transitional flows. A detailed engineer’s report, which provides information on the nature and consequence of the event, has been used to develop a test case. The report also includes a surveyed flood extent of the events, which allows quantification of model results, and provides a means for indentifying the levels of physical representation required to model a canal embankment failure. The test case is implemented by testing 4 LISFLOOD modules across a range of input parameters in a systematic, Monte Carlo style ensemble approach, and using a number of methods to assess the outputs.

2. LISFLOOD-FP

The LISFLOOD code contains several modules with different levels of physical representations, which provides an ideal framework for testing the impact. The framework is a 2D regular gridded model, which uses common boundary conditions and spatial discretization methods between codes. Consequently, variations between results can be attributed to the numerical model of the module. This overcomes issues that have impacted previous benchmarking studies, where using multiple computational codes to compare approaches can often reduce the clarity of the variations attributed to physical representations.

Initially LISFLOOD was produced as being a simple raster based model, in order to model floods with a minimal amount of computational effort. The model is a 2D finite difference model, based on the storage method where the floodplain is discretized into regular, square grid cells, where the depth of water in a grid cell is estimated by a calculation of the discharges moving in and out of the cell over a timestep. The initial code was based on a diffusive wave approach using the Manning’s equation as an inter-cell flux, providing an analytical solution to the diffusion wave (Bates and De Roo, 2000). It cannot be considered a numerical solution to the diffusive wave as the x and y components of the model are decoupled. An automatic time step procedure based on the quadratic of the grid cell size was developed that ensured that the module produced realistic solutions (Hunter 2005). Whilst this method produced reliable results, the application of it to urban environments, which require smaller grid cells in order to accurately capture the topographical detail, proved difficult. The use of the time step can be prohibitively small and force model run time to exceed in some cases several days. This approach provides a diffusion wave approach with low mass errors indicating a robust methodology.

2.1 LISFLOOD-ACC

LISFLOOD-ACC represents a re-worked formulation of the momentum equation (Bates et al., 2010). This provides a greater representation of the physics of fluid motion in the flood plain. The numerical model at the centre of this module a quasi linear one dimensional form as;

$$\frac{\partial Q}{\partial t} + \frac{gA\partial(h_t + z)}{\partial x} + \frac{gn^2 Q^t}{R^{4/3} A} = 0 \quad [1]$$

Where;

Q=discharge

t=time

A=cross section area

g = gravitational constant

h= water free surface height

z = bed elevation

n = Manning’s coefficient

R = Hydraulic Radius

Where the first term represents the advection acceleration term from the momentum equation, the second term is the water slope, and the final term is friction slope value, equivalent to the S_f term determined in the LISFLOOD-ATS approach. The numerical solution does not require the adaptive time step as in ATS, and the Courant condition can provide a suitable timestep. The above formulation is not a traditional formulation of the equation being neither the full dynamic solution or as simplistic as the diffusive approach. Whilst the concept behind the model was to improve the time stepping used in ATS, it has the ability to represent more complex flows and to preserve momentum compared to the ATS module (Neal et al., 2011). This is a useful feature in respect of this study, as it provides a bridging solution between the full shallow water equations and the simpler diffusion approach.

2.2 LISFLOOD-Roe

LISFLOOD-Roe solves the full shallow water equations using Roe's approximate Riemann Solver to calculate, inter cell flux values. The numerical scheme is based on the full dynamic solution of the momentum equation. Using the same quasi linear one dimensional notation the full equation appears as;

$$\frac{\partial Q}{\partial t} + \frac{\partial}{\partial x} \left[\frac{Q^2}{A} \right] + \frac{gA\partial(h_t + z)}{\partial x} + \frac{gn^2 Q^t}{R^{4/3} A} = 0 \quad [2]$$

Where the second term represents advection forces and is not present in the LISFLOOD acceleration module. This approach has been applied to a storage cell method previously (Villanueva and Wright, 2006).

2.3 LISFLOOD-Rusanov

A second full SWE module is presented here. The Rusanov module uses the all the terms from the momentum equation as the LISFLOOD-Roe module, but uses the Rusanov solver to solve the Riemann problem at the intercell flux. In comparison to the Roe solver, which uses a approximation to the Jacobian matrix to sample a linear approximation for the intercell variables, the Rusanov flux determines the extreme values of the wave structure of the intercell flux to determine the local wave speed. The Rusanov approach is computationally cheaper as the maximum local wave speed can be determined from the same variables that are used to estimate the time step values. However, the compromise with this method is a flux which creates a large amount of numerical diffusion. By comparing this module with the LISFLOOD-Roe module, insight can be gained into the significance of the numerical solution as well as the level of physical representation.

3. METHODOLOGY

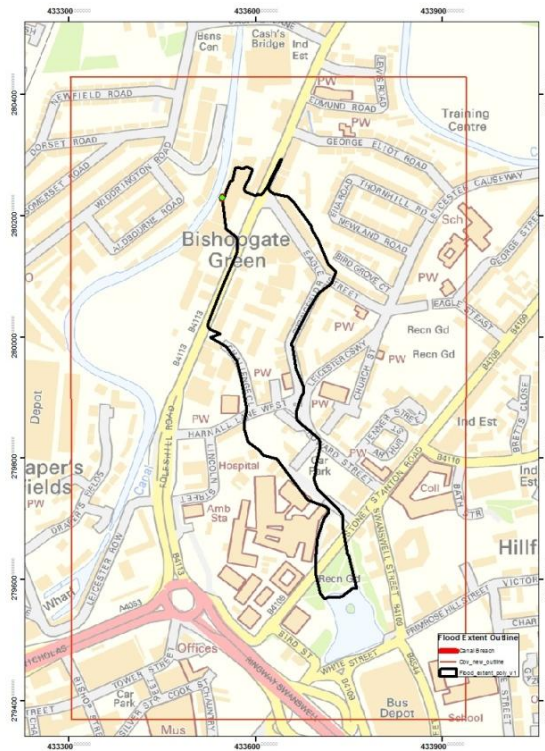


Figure 1: The test case region, and the outline of the flood extent

A systematic analysis of all model factors was undertaken for a case study in Coventry. The case study is based on a historic event that occurred in 1978, where part of the canal embankment failed as a result of building work that occurred in the area. The outpour inundated a 1km² inner urban area, which included the main hospital for the city, houses, and industrial units. The hydraulics of a canal embankment failure are dependent on a number of physical characteristics of the canal and the location of the embankment failure point relative to other features in the canal. The outflow is restricted by the difference between the base of the canal and the ground level, which reduces the amount of water in the hydrograph outflow compared to a dam failure scenario (Dun and Wicks 2013). Using the outflow methodology as used by Dun and Wicks (2013) the estimated outflow contained a peak discharge value of 20m³/s, which occurs 5minutes after the initial outburst. The hydraulics of the case study are characterized by an immediate outburst, which is supercritical for the initial stages. A main flow path occurs running north to south along the road network. The topography is well defined in this region, with a low slope running north to south and a well constrained depression which plays a significant control on flow. The flow path eventually terminates at a pond from which the canal waters disperse to the natural water system.

The input factors are summarized in Table 1. The uncertainty ranges for each input factor are based on values typically used in modeling studies. Friction parameters are based on a literature values of Manning's coefficient (Chow et al 1988) and expanded to include a range of potential values (Hunter et al 2008) 2 main approaches were used, a spatial distributed value where friction values were based on underlying land use classification and a uniform value over the entire model domain. The uncertainty associated with implementation of friction values can therefore be assessed.

Parameter Type	Range	Notes
Cell Size	2m – 4m for urban tests	Based on work by Fewtrell et al (2008)

Hydrograph	20% of calculated hydrograph	Value based on Brandimarte et al (2010)
DEM error	15cm	LiDAR vertical RMSE
Building Representation	BH, BR, BP, BB	Based on Schubert and Sanders (2012)
Friction Value	0.08-0.020	Manning's n for low friction
	0.015-0.075	Manning's n for high friction
	0.01-0.07	Uniform friction values

Table 1: Input parameters for the test case

The range for the uncertainty on the hydrograph is based on a value of 25% which represents the estimated value for hydrographic uncertainty (Brandimarte et al. 2010). This also represents the bands of uncertainty for the estimated hydrograph outflow.

In order to replicate the event, a 2008 LiDAR Digital Elevation Model, was altered to represent the land coverage in 1978. The underlying digital surface model is retained, although the road network has been altered by digitizing the 1970 data, and increasing the depth of the DSM where the road data overlays the by 0.1 meter. The grid cell size was then resampled and tested at 2m and 4m resolution to represent a range of potential grid size values that could be used to accurately model urban areas (Fewtrell et al 2008). This sample investigates a common problem in modeling, the link between computational efficiency and representation of flow processes. A further uncertain component represented in the test case relating to the DEM, is the vertical and horizontal root mean square error (RMSE) of the LiDAR, of 15cm (Cobby et al 2001). The resample DEM was then degraded randomly by the RMSE to represent the impact of the RMSE on the sampled elevation value. Two DEM's are therefore used to test the impact of this, in a similar process to Hunter et al (2008) and Tsubaki et al (2013).

The uncertainty relating to the methods of representing buildings in the model domain has been explored (Sanders et al 2012, Schubert et al 2008). Three methods of building representation were used in this test case. Building Block (BB) method where the elevation in the footprint of the building is raised by 6m above the surface elevation. Two methods, which allow water to flow through the buildings were also used. The first is a Building Resistance method (BR), where a higher friction value of 0.1 is assigned to the footprint of the building. A Building Porosity (BP) model was also used, whereby the building is not explicitly represented, but a porosity model is used in the cells of the building footprint. A similar porosity model to Sanders et al (2008) is used. A fixed conveyance porosity level is used across all the BP models

The model results are assessed in two methods, the first is a typical model assessment method that uses the widely used F^2 method (Aronica et al 2002). The second methodology is a cost of damage method to estimate the financial impact of the event. This method was implemented by determining underlying building type from the OS data, and assigning a depth damage curve from the Multi Colored Manual (MCM) to determine the cost of damage to an building (Penning-Rowsell et al 2005). The depth was determined from the cells that surround the building to allow the multiple building representation types to be compared. 5 categories were used, which represent the broad range of building types in the area.

4. RESULTS

Each input factor was cross compared and evaluated with the above methods. Probabilistic plots of the maximum extent for each model realisation of the module are displayed in Figure 2. This figure is based on the approach used by Aronica et al (2002), where dark regions represent cells that have flooded in all scenarios, and grey regions cells that have flooded in some model realisations. Each module appears to replicate the main outflow characteristics of the event described in the engineers report of the event. A

main flow path emerges north to south, with lower depth flow emerging off the flowpath. Overall, the probabilistic outlines provide a number of insights into the influence of module choice and key controls on the flood extent.

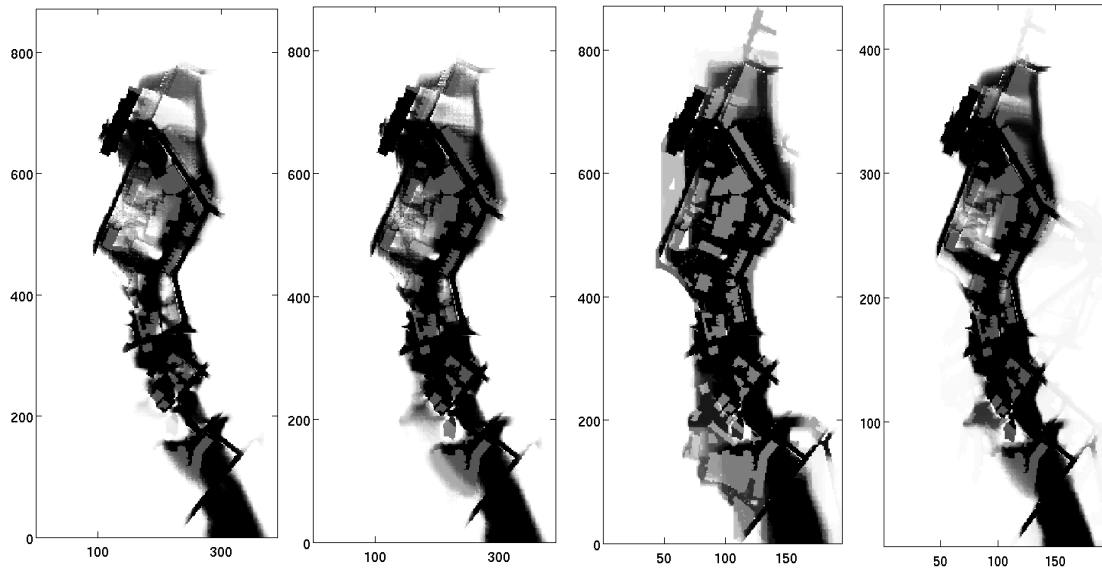


Figure 2: Probabilistic outputs for the 4 modules across the parameter space, from left to right ATS, ACC, Rusanov, Roe, where dark regions represent cells that have flooded in all model realisations and where dark regions represent cells that have flooded in all test cases

Each plot appears to be similar in extent and width. This suggests that simplified approaches are just as valid in replicating the flood extent in complex urban areas as the full SWE models. Furthermore, there are fewer uncertain regions, represented by the grey areas on the flood extents for the four modules. This indicates a relative insensitivity to the other parameters in the test case, and indicates that underlying topographic controls are more significant in determining the extent of the flood. A number of small variations though, provide insight into how the levels of physical representation impact model results. A region located at the top of the model domain (between 200-300 meters and 600-800 meters) varies between each module in terms of extent, and likelihood value. For the simplified modules, this region has a smaller extent and lower probability value, in comparison to the full SWE modules, which are both wider, and have higher probability. This is related to the fact that the addition of the convective and local acceleration terms in the full SWE modules allows the flood wave to overcome many of the urban obstacles in the model domain. This impact is subtler here than in the Glasgow benchmarking study of Hunter et al (2008), but the effect and variation is similar.

This insensitivity to other parameters and the similarity of results between different levels of physical representation are further enforced in a comparison of the binary extent of the modeled extent versus the surveyed observed extent. The comparison is made using the F^2 value (Aronica et al 2002) and is a method that has been traditionally used in analyzing model results. A summary of the results are made in Table 2.

Model(function)	ATS	ACC	Rusanov	Roe
F^2 (Mean)	0.635	0.618	0.550	0.601
F^2 (Max)	0.710	0.687	0.673	0.687

F² (Min)	0.511	0.464	0.402	0.332
----------------------------	-------	-------	-------	-------

Table 2: Summary of results from the test case

The ATS module produces the highest F² value, as well as the highest mean value. By comparison the Rusanov solver produces the lowest maximum value of F². The range of values from each of the modules is summarized in the box and whisker plot of Figure 3, and indicates that the range of results from each module is low, with the exception of the Rusanov code, which is sensitive to the value of friction coefficient as a result of the simplified numerical approach of the numerical code. With the exception of the Rusanov code, a gradual decrease in the mean value of F² for each module can be observed, which indicates that with increasing physical representation lower values of F². This seems to contradict previous work, which suggests that higher levels of physical representation improve model result.

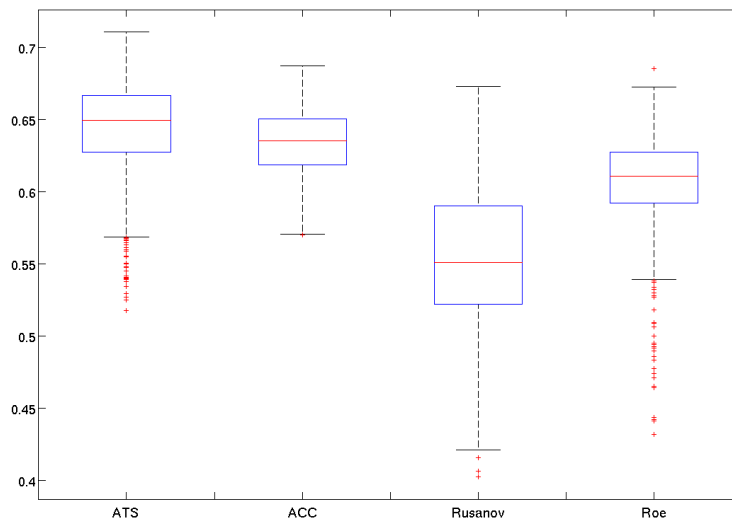


Figure 3: Box plot of the F² value for each module

Part of the explanation for this is due to the how well each module defines the main flowpath. For the modules with higher levels of physical representation, the flood waters can overcome the urban topography, setting up secondary flow paths which increase the inundation extent, and consequently increase the number of over predicted cells, which can reduce the F² value. A further point is the uncertainty related to the surveyed data extent. Details of the precise surveying methods, the physical feature that was observed and the time from the event, all of which affect the accuracy of the observed data set are not recorded in the engineer's report of the event. The region of greatest variation between the module, discussed earlier in this section, is significant in terms of affecting the modeled extent, but in terms of depth and consequently risk is less critical. It can be assumed that this water may have dried up or not be considered of great significance in determining the final surveyed level of water.

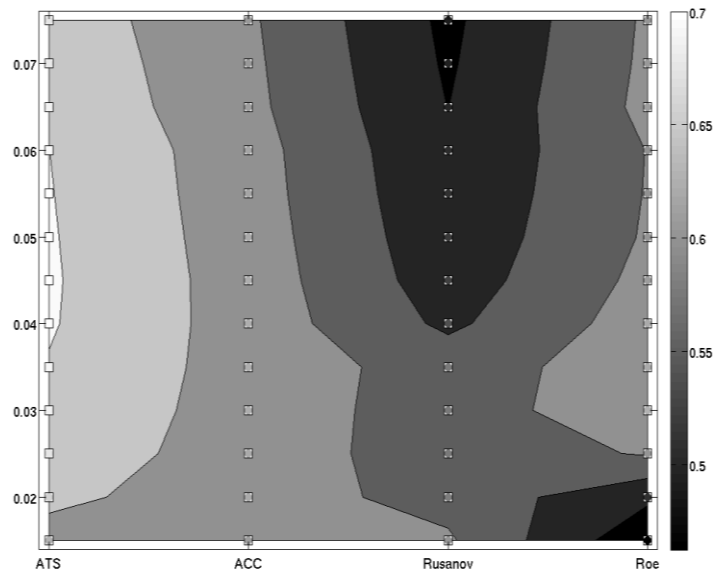


Figure 4. The F^2 value plotted over the module/Manning's friction parameter space. Darker values represent lower values of F^2 . The model results are represented by discrete markers. The contours are to allow for easier visual comparison.

The impact of other parameters is less critical, but still displays important first order interactions, and provides evidence of higher order interaction between parameter sets. Plotting the F^2 value over the parameter space of level of physical representation versus the value of friction parameter indicates that the gradient of F^2 value, and therefore the significance of the input factor is greatest across the module type. The gradient however is not uniform, with distinct variations of the gradient relative to the friction choice, in particular the variation of the Rusanov and Roe solvers which show an inverse relationship relative to each other. This interaction demonstrates the complexity of the parameters space as well as determining the relationship between model inputs. This analysis is further in figure ??, where for each level of input, the mean value is determined and compared to mean values for other factors. The interaction plot allows the analysis of multiple, and key factors and relationships can be determined from the gradient of the line where a steeper gradient for each factor indicates first order interaction significance, whilst crossing lines in each box indicates higher order interaction. Overall, the most significant input is the model type (first column, and first row), where the gradient and variation of the line across the other parameters indicates the importance of these terms. The relative lack of gradient for other parameters, in particular the cell size, hydrograph and DEM error indicate low importance as inputs. The higher order impact of friction type can be determined from the square of row 1 and column 3, where the mean value between modules diverges at higher friction values. Again it is noted that even for important factors, the variation between the model input ensemble is relatively low, with all models seemingly able to replicate the observed extent to a reasonable standard. This represents the classic equifinality issue in environmental modeling (Beven and Bingley 1992).

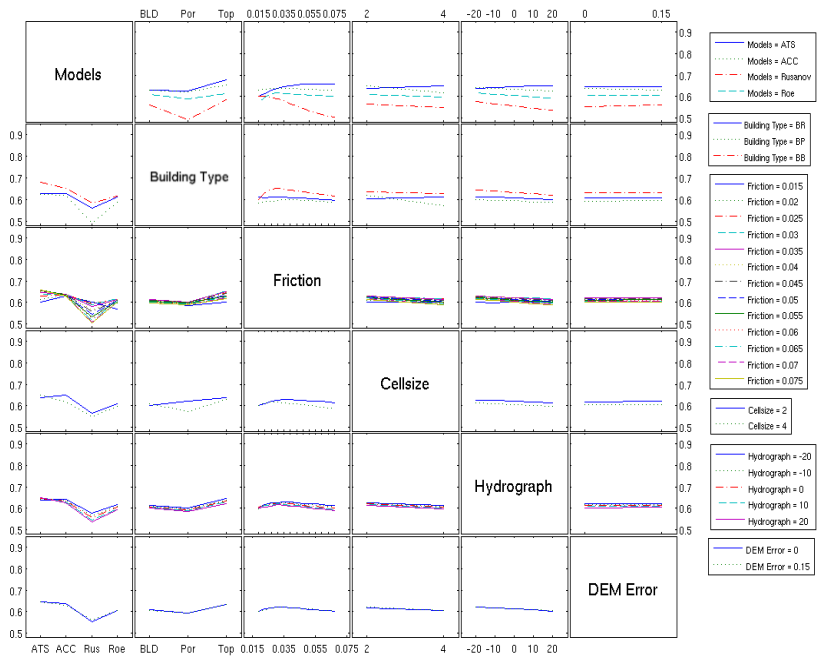


Figure 5: Interaction plot for each input factor comparing mean value of F^2 per level of factor other levels of factors.

The indication from the flood extents and measure of F^2 that the level of physical representation and other parameters are relatively unimportant factors in affecting model outputs and that underlying terrain data is more significant. Detailed analysis of modelled depths indicates a significant difference for each of the modules. For a point located in the center of the model domain and along one of the main flow paths that emerge from the canal outflow, the variation between each module is apparent.

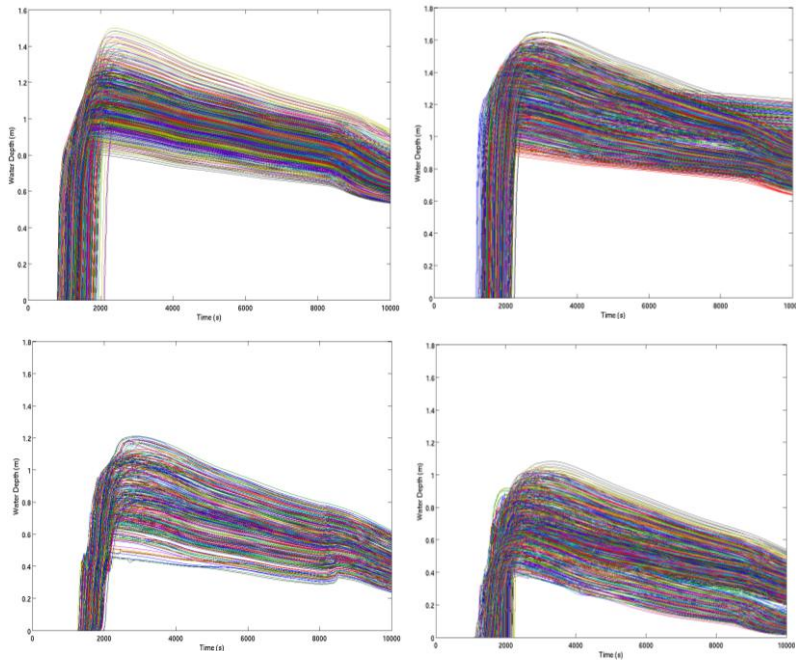


Figure 6: Water depths for the 4 modules over the range of tests

A number of points can be determined from this. First, the time from initial inundation to peak value is relatively short, around 2 minutes across the model results for each parameter space, but varies considerably between each module. For the simplified approaches, the time to peak value from arrival is very short at around 100-200 seconds, whereas the full dynamic wave models are around 200-300 seconds. Second, the value of peak also varies considerably between the modules and this can be attributed to the ability to represent transcritical flow in the full SWE modules, whereby water is moved through at a greater amount due to the higher velocities associated with supercritical flow. Peak depth values for the Rusanov and Roe modules are significantly lower than the simplified models, around 0.8m lower, which is a product of both the transcritical flow conditions, where high velocities for water depths are encountered, and the ability to flood a wider extent, providing less water to the main flowpath. The timing of initial inundation for this control point also varies considerably between each module. The ATS module produces the earliest arrival time, and the widest range of arrival times, in comparison to the other modules, which produce similar values. The ATS module mean value of 22 minutes compares to 30 minutes for the ACC module and 28 minutes for the full SWE modules. The indication here is that the diffusion wave approach provides a well defined main flow path that channels the water effectively through the model domain. This is further developed by using probabilistic hazard plots, which display the regions where combined water depth and velocity exceed 0.7, above which flood waters are considered hazardous to health (DEFRA 2007). A similar approach to the probabilistic extent plot is used, defining regions of high likelihood across the model ensemble in darker red, and it is developed from the approach used by Aronica et al (2012). A clear pattern can be discerned between the simplified approaches and the full SWE, where the diffusive wave approach clearly replicates the main flow path across the model ensemble, which can be seen to be a dark red band running central to the model domain. As the level of physical representation increases, the definition of the secondary flow paths increases. This demonstrates that simplified approaches can significantly under estimate hazard.

For the full SWE modules, the majority of the domain is considered hazardous. The Rusanov module also shows large areas of high likelihood value, over a wide extent. This represents an over estimation of the flood hazard, as no issues relating to the outflow are reported in the engineers report of the event. This is in part due to the tendency of the module to overestimate the velocity of the initial outburst, particularly in low friction value modules. This is a potential issue with the Rusanov solver and other simplified methods, which can prove to be unstable in transcritical conditions where maximum wave speeds will increase, and potentially cause the wave front to produce higher velocities, which are then used in the calculation of hazard. The spatial distribution of value of likelihood for the Roe solver by comparison indicates though a large amount of uncertainty occurs from the model results. The main flow path contains high likelihood values, as does the secondary flow paths indicating that at this level of numerical solution and physical representation the main regions of risk are consistently replicated across the parameter space, increasing the confidence with which conclusions about areas of high risk can be made from this module. The issue of the wider flood extent in the middle section of the domain is also not highlighted as being critical to overall hazard likelihood values. The larger extent for the Roe solver in the lower regions of the model domain are caused by low friction value models and high hydrograph values (0.015 and +20% of the calculated hydrograph). This indicates that some models are over estimating risk, but also demonstrate that using hazard based approaches can be used to refine the model calibration process. Furthermore, this hazard mapping indicate that the use of extent alone under estimates the total hazard value, which may be critical if model output is extended beyond the use of simple extent comparisons to determine the risk associated with flooding.

The implication here is that local variation between modules is not sufficiently captured by the simple comparison of F^2 . By incorporating vulnerability measures in the model evaluation process, in particular a cost of damage which is based on evaluating depths/damage curves for cells adjacent to buildings, the effect of uncertain parameters can be evaluated further.

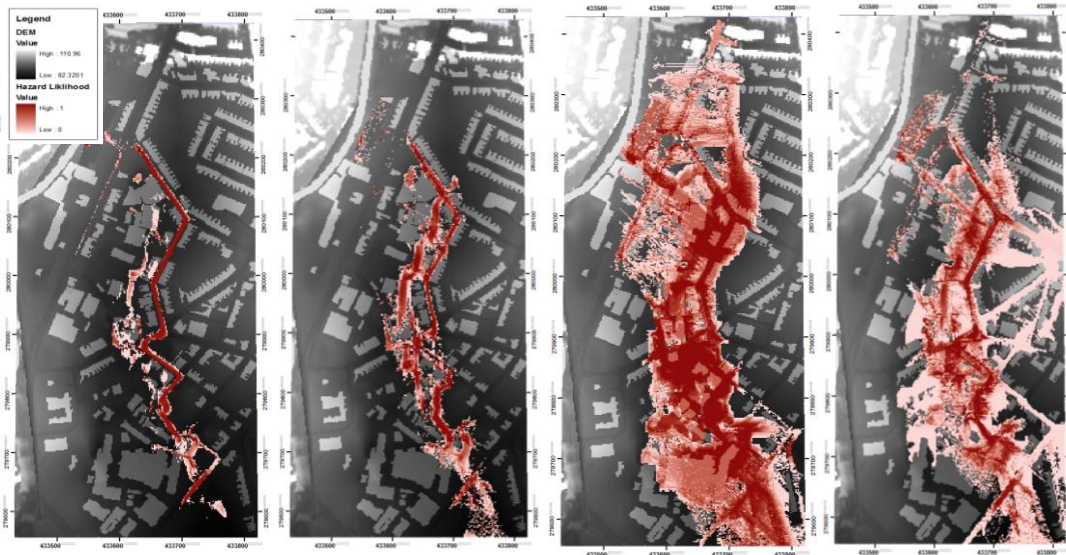


Figure 7: Probability plots for regions of hazard, where red regions represent the high hazard areas, from left to right ATS, ACC, Rusanov, Roe, where dark regions represent cells that have flooded in all model realisations.

Using a cost of damage method has two distinct advantages as a as a measure of model output. First it allows effective communication of model outputs to decision makers, translating direct model output into a format widely understood by non technical specialists. Further to this point, the buildings and values of interest can be determined by decision makers, allowing calibration and model output to be focused on key regions. Secondly, this method allows key local variations to be incorporated into a single value model descriptor. Using OS data to determine building type and footprint, and assigning a depth/damage curve from the Multi Colored Manual (MCM), each model realization was assessed. In the absence of appropriate validation data, the variance between each model, and the total cost are considered. The results are summarized in table 3.

Cost of Damage (£)	ATS	ACC	Rusanov	Roe
Mean	12372031	14328383	13086956	13156250
Min	9134556	10381984	9050304	9460980
Max	16714196	18280158	17723138	18209052
Standard Deviation	1763212	2041334.9	1921726.7	2068624

Table 3: Summary results of the cost of damage for the 4 modules.

Analysis of this data shows a number of characteristics are retained from the F² analysis, such as the highest cost values being replicated by a simplified module, in this case the ACC, which regularly

produces higher depths, albeit at a later arrival time. This output which can be seen clearly in the analysis of water depths is implicitly captured in the model result, indicating the advantage of using such an approach for evaluating models. A key difference is that the difference between the modules is lower than in comparison to the F² method. Each module produces a similar range of costs across the range of models. This is in part due to the majority of critical buildings being flooded to a similar level across all module types. The spatial distribution of water is less critical, as the majority of at risk buildings lie within the constrained basin of this test case. The variation between model results are however greater, which leads to easier discrimination between best performing models. The ability of a calibration technique to provide a greater peak in the assessment of model results is critical in providing robust analysis of model output. It is anticipated that where data that relates to the cost of event is available, model calibration would be more powerful than by using observation data.

5. DISCUSSION AND CONCLUSIONS

The Coventry test case is unique both in the type of event, which can be classified as a low occurrence probability, high impact event. The restrictive topography, relatively small model domain and the unique hydraulic properties provide a useful examination of the LISFLOOD-FP code and modules. The highest goodness of fit value was returned by the ATS module, while increasing levels of physical representation appear to reduce this function. Further examination by the use of water and velocity hazard measure have highlighted not only how this value can potentially be misleading, it can also lead to an under prediction of the hazard. The results also indicate the requirement to use connected sewage networks when modeling outburst events in urban regions. A significant assumption made in the use of flood inundation models in urban environments is the surcharging of drains. This test indicates that for certain scenarios this may not be valid, in particular for the region of the modeling domain, where variation between the modules was greatest. This confirms previous findings that identify the uncertainty in using extent observation to calibrate model realizations (Stephens et al 2012). Overall, the level of physical representation appears to be the most influential in determining model results, but that this influence is non linear. In this test case, the overall trend is for the ATS and ACC results to be markedly different than the full SWE modules and the variation between the simplified approaches also demonstrate variations. This indicates that assumptions about appropriate levels of physical representation may be difficult to quantify, but the impact maybe critical overall. The use of hazard based approaches can help to reduce the level of uncertainty through spatial analysis and model comparison analysis.

6. REFERENCES

- Aronica, G., Bates, P. D. & Horritt, M. S. 2002. Assessing the uncertainty in distributed model predictions using observed binary pattern information within GLUE. *Hydrological Processes*, 16, 2001-2016.
- Beven, K. & Binley, A. 1992. The Future Of Distributed Models - Model Calibration And Uncertainty Prediction. *Hydrological Processes*, 6, 279-298.
- Bates, P. D. & De Roo, A. P. J. 2000. A simple raster-based model for flood inundation simulation. *Journal of Hydrology*, 236, 54-77.
- Bates, P. D., Horritt, M. S. & Fewtrell, T. J. 2010. A simple inertial formulation of the shallow water equations for efficient two-dimensional flood inundation modelling. *Journal of Hydrology*, 387, 33-45.
- Brandimarte, L. & Woldeyes, M. K. 2013. Uncertainty in the estimation of backwater effects at bridge crossings. *Hydrological Processes*, 27, 1292-1300.
- Cobby, D. M., Mason, D. C. & Davenport, I. J. 2001. Image processing of airborne scanning laser altimetry data for improved river flood modelling. *Isprs Journal of Photogrammetry and Remote Sensing*, 56, 121-138.

- Dun R, & Wicks J. 2014. Canal breach risk assessment for improved asset management *Proceedings of the ICE - Water Management*, 167, 1, 5-16.
- Environment Agency Science Report (2009) SC080035/SR, Desktop review of 2D hydraulic modelling packages
- Fewtrell, T. J., Bates, P. D., Horritt, M. & Hunter, N. M. 2008. Evaluating the effect of scale in flood inundation modelling in urban environments. *Hydrological Processes*, 22, 5107-5118.
- Fewtrell, T. J., Duncan, A., Sampson, C. C., Neal, J. C. & Bates, P. D. 2011. Benchmarking urban flood models of varying complexity and scale using high resolution terrestrial LiDAR data. *Physics and Chemistry of the Earth*, 36, 281-291.
- Hall, J. W., Tarantola, S., Bates, P. D. & Horritt, M. S. 2005. Distributed sensitivity analysis of flood inundation model calibration. *Journal of Hydraulic Engineering-Asce*, 131, 117-126.
- Hunter, N. M., Bates, P. D., Neelz, S., Pender, G., Villanueva, I., Wright, N. G., Liang, D., Falconer, R. A., Lin, B., Waller, S., Crossley, A. J. & Mason, D. C. 2008. Benchmarking 2D hydraulic models for urban flooding. *Proceedings of the Institution of Civil Engineers-Water Management*, 161, 13-30.
- Neal, J., Villanueva, I., Wright, N., Willis, T., Fewtrell, T. & Bates, P. 2011. How much physical complexity is needed to model flood inundation? *Hydrological Processes*, 26, 15.
- Pappenberger, F., Beven, K. J., Ratto, M. & Matgen, P. 2008. Multi-method global sensitivity analysis of flood inundation models. *Advances in Water Resources*, 31, 1-14.
- Penning-Rowsell E., Priest S, Parker D, Morris J., Tunstall S., Viavattene C., Chatterton J., Owen D., (2010) *Flood and Coastal Erosion Risk Management: A Manual for Economic Appraisal* Routledge
- Stephens, E.M, Bates P.D, Freer, J.E., Mason D.C, 2012 The impact of uncertainty in satellite data on the assessment of flood inundation models *Journal of Hydrology* 414, 162-173
- Sanders, B. F., Schubert, J. E. & Gallegos, H. A. 2008. Integral formulation of shallow-water equations with anisotropic porosity for urban flood modeling. *Journal of Hydrology*, 362, 19-38.
- Schubert, J. E. & Sanders, B. F. 2012. Building treatments for urban flood inundation models and implications for predictive skill and modeling efficiency. *Advances in Water Resources*, 41, 49-64.
- Tsubaki, R. & Kawahara, Y. 2013. The uncertainty of local flow parameters during inundation flow over complex topographies with elevation errors. *Journal of Hydrology*, 486, 71-87.